Elucidating the degradation mechanism of a self-degradable dextran-based medical adhesive

Woogi Hyon[a,b], Shuji Shibata[b], Etsuo Ozaki[b], Motoki Fujimura[b], Suong-Hyu Hyon[b], Kazuaki Matsumura*[a]

a. School of Materials Science, Japan Advanced Institute of Science and Technology
1-1 Asahidai, Nomi, Ishikawa 923-1292, Japan
b. BMG Incorporated,
45 Minamimatsunoki-cho, Higashikujo, Minami-ku, Kyoto 601-8023, Japan

* Corresponding author: Kazuaki Matsumura
E-mail: mkazuaki@jaist.ac.jp
TEL: +81-76-51-1680
FAX: +81-76-51-1149

Abstract

We developed a self-degradable medical adhesive, LYDEX, consisting of periodate-oxidized aldehyde-functionalized dextran (AD) and succinic anhydride-treated ε-poly-L-lysine (SAPL). After gelation and adhesion of LYDEX by Schiff base bond formation between the AD aldehyde groups and SAPL amino groups, molecular degradation associated with the Maillard reaction is initiated, but the detailed degradation mechanism remains unknown. Herein, we elucidated the degradation mechanism of LYDEX by analyzing the main degradation products under typical solution conditions *in vitro*. The degradation of the LYDEX gel with a sodium periodate/dextran content of 2.5/20 was observed using gel permeation chromatography and infrared and ^{1}H NMR spectroscopy. The AD ratio in the AD-SAPL mixture increased as the molecular weight decreased with the degradation time. This discovery of LYDEX self-degradability is useful for clarifying other polysaccharide hydrogel degradation mechanisms, and valuable for the use of LYDEX in medical applications, such as hemostatic or sealant materials.

Keywords
hydrogel, LYDEX, degradation, dextran, poly-L-lysine, Maillard reaction.

1. Introduction

Surgical tissue adhesives are commonly used as sealants to stop bleeding from organs and tissue sutures and prevent air leakage from cut surfaces during thoracic surgery. Tissue adhesives composed of natural or synthetic polymers, or a combination, have been developed (Li et al., 2014). Fibrin-based sealants are highly biocompatible due to their blood coagulation properties, but weak adhesive strengths (MacGillivray, 2003) limit their applications, with the risk of viral infection also reported (Canonico, 2003; Hino et al., 2000; Ortel et al., 1994; Siedentop et al., 2001; Silver et al., 1995). Conversely, cyanoacrylate, a synthetic adhesive, exhibits high stiffness and adhesive strength, but inhibits *in vivo* healing of the diseased area due to systemic inflammatory reactions (Ramond et al., 1986) and high cytotoxicity (Bhatia et al., 2007). This is because of the involvement of aldehyde compounds in the gelation and degradation of the adhesive. Hence, their areas of application are limited, and they cannot be used in direct contact with the central nervous system or blood vessels. The combination of natural and synthetic polymers is represented by adhesives that contain gelatin cross-linked with formaldehyde and glutaraldehyde. Although the adhesive strength is sufficiently high, the preparations of these adhesives include toxic aldehyde compounds as cross-linking agents (curing components), with their use limited by their biotoxicities (Erasmi et al., 2002; Fürst & Banerjee, 2005; LeMaire et al., 2002).

As none of these are ideal tissue adhesives for repairing damaged elastic and soft tissues, extensive research and development has recently been conducted to design biocompatible, biodegradable, flexible sealants to form leak-free seals in soft tissues.

Elvin et al. reported that a photocrosslinked fibrinogen-based hydrogel based on Ru-catalyzed photooxidation of tyrosine residues (Fancy & Kodadek, 1999) showed improved adhesion strength, extensibility, and tensile strength compared to those of previously approved products (C. M. Elvin et al., 2010; Christopher M. Elvin et al., 2009). Elvin et al. synthesized a photocrosslinkable gelatin sealant via a similar reaction and observed the blood and air leak prevention effects in lung tissue using a sheep model (Christopher M. Elvin et al., 2010). Taguchi et al. reported an improvement in the pressure resistance by introducing dodecyl groups into pollock-derived gelatin to increase hydrophobic interactions (Mizuno et al., 2017). Several types of sealants have been developed using albumin, such as gelatin, from various animal sources. For example, the United States Food and Drug Administration approved BioGlue (CryoLife, Inc.) (Chao & Torchiana, 2003) consisting of bovine albumin and glutaraldehyde, and Progel (Daboll, Inc.) (Fuller, 2013; Kobayashi et al., 2001), a composite sealant containing human albumin and a polyethylene glycol (PEG) cross-linker with two NHS-activated ester groups. When the two components are mixed, the primary amine group of the albumin lysine residue reacts rapidly with the succinimidyl succinate group to form a cross-linked structure within 1 min.

Research regarding sealants containing polysaccharides, which are widely used in medicine and food as natural polymers, is also active. As sealants, chitosan derivatives were prepared by reacting chitosan with lactobionic acid in the presence of water-soluble carbodiimide (Ishihara et al., 2002; Ono et al., 2000). Moratti et al. reported the hemostatic and adhesive properties of gels consisting of succinylated chitosan and dextran aldehyde (Liu et al., 2009). Imine bonds are formed between amino and aldehyde groups, yielding gels. Elisseeff et al. reported a gel-based sealant consisting of chondroitin sulfate with aldehyde groups combined with poly(vinyl alcohol-*co*-vinylamine) (Reyes et al., 2005).

Polyurethane- (Gilbert et al., 2008), PEG- (Hill et al., 2001; Wallace et al., 2001), and polyester-based (Sakai et al., 2013) synthetic sealants have been developed as wound closure technologies suitable for clinical applications, owing to their excellent adhesion strengths and tunable mechanical properties.

Additionally, we developed a novel dextran-based self-degradable medical adhesive, LYDEX, which exhibits high adhesive performance and flexibility, low toxicity, and no risk of viral infection, to meet clinical requirements (Araki, Tao, Nakajima, et al., 2007; Araki, Tao, Sato, et al., 2007; Hyon et al., 2014; Matsumura et al., 2014). LYDEX is prepared using natural dextran and ε-poly-L-lysine (ε-PLL) polymers. In addition, as various dosage forms (liquid, powder, sheet, and disc) may be selected, numerous medical applications have been studied, including hemostatic (Naitoh et al., 2013; You et al., 2014), sealant (Araki, Tao, Nakajima, et al., 2007; Araki, Tao, Sato, et al., 2007), and anti-adhesion materials (Kamitani et al., 2013; Takagi, Araki, et al., 2013; Takagi, Tsuchiya, et al., 2013), and endoscopic wound dressing (Bang et al., 2019).

Dextran within LYDEX predominantly consists of α-1,6-linked glucose polymers synthesized by the heterolactic acid bacteria *Leuconostoc mesenteroides*. Dextran is widely applied in the biomedical field because of its biocompatibility (Cadée et al., 2000; Ferreira et al., 2004), low toxicity (Hyon et al., 2014), simple modification (Mehvar, 2000), and enzyme-mediated degradability *in vivo* (Khalikova et al., 2005). In addition, dextran contains numerous hydroxyl groups, which provide high hydrophilicity and may be used in chemical functionalization (Lévesque & Shoichet, 2007; Maia et al., 2005; Massia & Stark, 2001; Matsumura & Rajan, 2021; Mehvar, 2000).

To develop LYDEX, we employed a modification strategy wherein sodium periodate was used to introduce aldehyde groups into dextran, which reacted with amino groups to form imine bonds (Schiff base), leading to hydrogel formation (Figure 1). Specifically, aldehyde-functionalized dextran (AD) was mixed with ε-PLL (Araki, Tao, Nakajima, et al., 2007; Araki, Tao, Sato, et al., 2007). This hydrogel showed *in vitro* degradation without degradable cross-linking points (Matsumura et al., 2014). In addition, the development of hydrogels as biomedical adhesives and scaffolds using aldehyde-modified polysaccharides by periodate oxidation (Malaprade reaction) (Malaprade, 1928) has been previously reported (Drury & Mooney, 2003).

Studies on LYDEX degradation are underway. The oxidative cleavage of dextran using sodium periodate (Malaprade reaction) (Malaprade, 1928) is long-known, with the ring cleaved to form two aldehyde groups accompanied by partial degradation of the main chain (Maia et al., 2005). The structure of oxidized dextran is diverse, not unitary, and an intermolecular hemiacetal model between three types of molecules was proposed, using NMR structural analysis (Drobchenko et al., 1993; Maia et al., 2005, 2011). We investigated the possibility of an intramolecular hemiacetal model based on the assumption that the aldo–enol transition occurred, as the proton of the aldehyde group of oxidized dextran was undetected using NMR spectroscopy (Chimpibul et al., 2016). In addition, oxidized dextran undergoes irreversible reactions with amino groups, resulting in cross-linking and gelation due to imine bond formation; when the Amadori rearrangement occurs, the 1,6-glycosidic bond becomes unstable and rapidly cleaves the C–O bond of the main chain adjacent to the imino group, resulting in a decrease in molecular weight (Mw) within an hour and swelling of the gel (Hyon et al., 2014; Maia et al., 2005, 2011). Subsequently, the partial hemiacetal structure generated by periodate oxidation reacts with amino groups and undergoes Amadori rearrangement, leading to the cleavage of the glucose unit ring and molecular degradation (Chimpibul et al., 2016) (Figure S1). A hydrogel exhibiting controlled degradation of dextran derivatives via this degradation

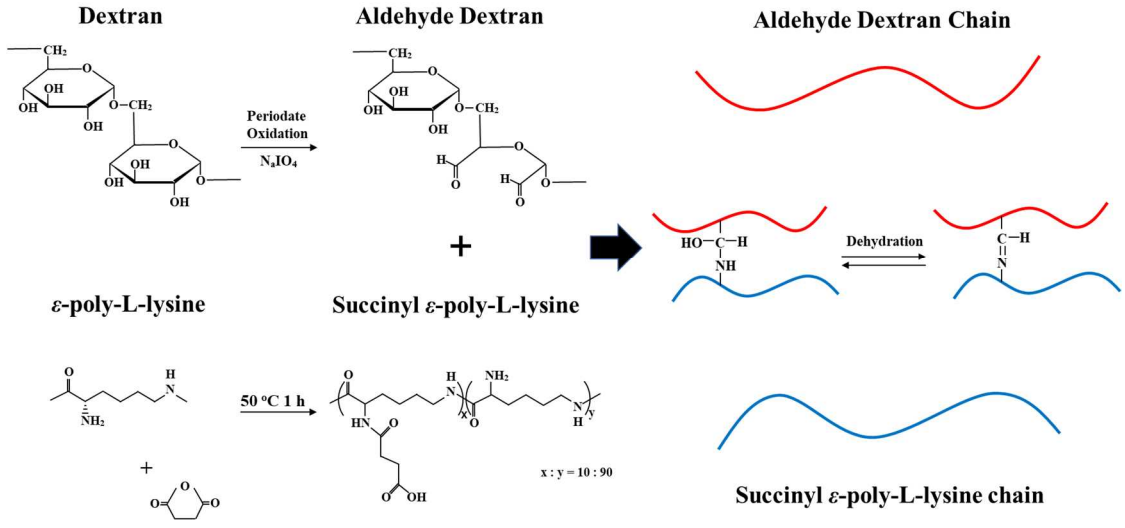

Figure 1. LYDEX hydrogel formation.

mechanism was designed and showed potential as a drug-releasing substrate (Nonsuwan et al., 2019; Nonsuwan & Matsumura, 2019). Furthermore, this degradation mechanism may be applied to induce molecular degradation of cellulose; oxidized cellulose is useful as a low-toxicity biodegradable scaffold (Chimpibul et al., 2020).

Although the gelation of the aldehyde of oxidized dextran and the amino groups is followed by the

Maillard reaction and molecular degradation, the degradation mechanism and products of LYDEX have not been fully elucidated. For clinical application, clarification of the degradation products, mechanisms, and *in vivo* kinetics is necessary to confirm their effects on biological safety. Furthermore, clarification of the *in vitro* degradation behavior of LYDEX is useful for elucidating the *in vivo* degradation and absorption mechanisms. Therefore, in this study, the main degradation products of LYDEX in aqueous media are analyzed experimentally to elucidate the degradation mechanism.

2. Material and methods

2-1. Materials

Dextran (70 kDa) was obtained from Meito Sangyo (Nagoya, Japan) and ε-PLL (4 kDa, 25 wt.% aqueous solution, free base) from JNC (Tokyo, Japan). Sodium periodate, succinic anhydride (SA), and other chemicals were purchased from Nacalai Tesque (Kyoto, Japan). All chemicals were used without further purification unless otherwise stated.

2-2. Preparation of AD

AD (oxidant/dextran ratio: 2.5/20 w/w) was prepared by oxidizing dextran with sodium periodate according to the method reported (Mo et al., 2000).

2-3. Preparation of SA-treated PLL (SAPL)

AD reacts with the primary amino group of ε-PLL at a neutral pH to form a hydrogel. To control this reactivity and due to its low toxicity (Chao & Torchiana, 2003), SA was used to synthesize SAPL. ε-PLL is an oligomer of the amino acid L-lysine with 25–35 primary amino groups per molecule, but SAPL consists of an α-carboxyl group bonded to an ε-amino group. Several amino groups of ε-PLL were acylated by SA addition according to a previously reported method (Hyon et al., 2014).

2-4. Characterization of AD and SAPL

2-4-1. Aldehyde content determination

The aldehyde content of AD was evaluated using a simple iodometric titration method used in a previous study (Hyon et al., 2014). Briefly, *ca*. 1% w/v aqueous AD solution (10 mL) was added to an I_2 solution (20 mL, 0.05 M), followed by NaOH addition (20 mL, 1 M). The oxidation reaction proceeded for 15 min. After H_2SO_4 addition (15 mL, 6.25% v/v), the I_2 consumption was determined by titration with 0.1 M $Na_2S_2O_3$ using one drop of 20% w/w starch solution as an indicator. The aldehyde group reacts with 1 mol of I_2 under alkaline conditions to form a carboxylic acid, and 1 mol of I_2 reacts with 2 mol of $S_2O_3^{2-}$ ions. Three readings were obtained for each titration (n = 3).

The aldehyde content (mol/ Aldehyde Glucose Unit (AGU)) was calculated using Equation 1.

$$\text{Aldehyde content} = \frac{C_{Na2S2O3} \times ([V_B] - [V_S]) \times Mw_{AGU} \times [D]}{[W] \times 2 \times 1000} \ (\text{mol/AGU}) \quad (1)$$

where [VB] is the titration volume of the blank, [VS] is the titration volume, [D] is the dilution rate of the sample, and [W] is the anhydrous-equivalent sample volume.

2-4-2. Carboxyl group content determination

The carboxyl group content in ε-PLL was evaluated using the ninhydrin method (McGrath, 1972). The acylated ε-PLL solution (10% w/v) was diluted 400-fold using distilled water, and subsequently, 0.1 mL of the dilution, 1 mL of ninhydrin solution (0.8 g ninhydrin and 0.12 g anhydrous hydrindantin in 30 mL 2-methoxyethanol), and 2 mL of acetic acid buffer solution (0.1 M acetic acid and 0.2 M sodium acetate, pH 5.5) were added to glass tubes, which were heat-sealed. After coloring at 100 °C for 3 min, the absorbance at 570 nm was recorded at 25 °C using an ultraviolet (UV)-visible spectrophotometer (UVmini-1240; Shimadzu, Kyoto, Japan). Three readings were obtained for each sample (n = 3). Separately, polylysine solution was colored using a ninhydrin solution and measured in the same manner. A calibration curve (aλ, bλ) was prepared using the obtained absorbances, and the residual amino group content is calculated using Equation 2.

$$R_{\text{amino}} = \left(\frac{A_\lambda - b_\lambda}{a_\lambda}\right) / c_{\text{SAPL}} \times 11 \div 10 \times 100 \quad (\%) \quad (2)$$

2-4-3. Preparation and degradation of LYDEX

LYDEX was prepared using AD powder, with an oxidant/dextran ratio of 2.5/20 (w/w), and SAPL powder in a 4:1 mass ratio. To prepare a LYDEX gel, 40 mg of LYDEX powder was added to the well of a silicone mold (φ: 10 mm, LADD Research Industries, Williston, VT, USA) with 60 μL of saline solution, and 120 μL of saline solution was added to form a hydrogel, which was allowed to stand for 3 min. To degrade the gel, the gel was removed from the silicone mold and placed in a brown glass bottle (30 mL, Nichiden-Rika Glass, Kobe, Japan) containing 12 mL of saline solution, and shaken for 1 d, or 1, 2, or 4 wk in a water bath shaker (37 °C, 100 rpm). This solution was then separated into filtrate and residue using a membrane filter (0.45 μm A045A047A, Advantech, Tokyo, Japan). The residue was washed with approximately 1 mL of water and dried under reduced pressure. The residue was weighed, and the filtrate was subjected to absorption spectroscopy using a Shimadzu UV-1800 spectrophotometer.

2-4-4. Degradation product analysis using gel permeation chromatography (GPC) fractionation and spectroscopy

LYDEX gels were subjected to degradation for 2 wk and filtered. The fraction of each GPC peak

was collected and analyzed. The sample volume used for preparative GPC was 5 mL, the injection volume was 100 μL per injection, and the number of preparative GPC runs was 50. TSKgel G4000PW_{XL} and TSKgel G2500PW_{XL} columns were used. Two milliliters of the obtained fractions were placed in dialysis tubes (Biotech CE Trial Kit, Repligen, Waltham, MA, USA; MWCO: 100–500D), immersed in approximately 1 L of ion exchange water at 4 °C, and gently agitated for approximately 20 h (during the ion exchange, the water was changed once). The dialyzed samples were placed in eggplant flasks, frozen in a freezer, placed in a desiccator (5 L capacity), and sublimated under vacuum (approximately 6 h). The remaining solids were collected and subjected to infrared (IR) and ^{1}H NMR spectroscopy. IR was performed using the KBr tablet method (4 mm φ) using an IRPrestige-21 (Shimadzu, resolution: 4 cm^{-1}, measurement range: 400–4000 cm^{-1}, cumulative number: 64 times), and ^{1}H NMR spectroscopy was conducted using a JNM-ECA 400 (400 MHz, JEOL, Tokyo, Japan). The lyophilized sample was dissolved in approximately 0.75 mL of D_2O (internal standard: none). Mw fractionation was performed using Shimadzu Prominence LC-20AD HPLC LC-Solution TSKgel G4000PW_{XL} and TSKgel G2500PW_{XL} columns, and absorption at 323 and 210 nm was measured using a UV detector, whereas refraction was measured using a differential refractometer. The Mw fractionation ranges of the columns ranged from 2000 to 300 000 Da for G4000PW_{XL} and <3000 Da for G2500PW_{XL} for PEG. Therefore, G4000PW_{XL} was used to examine the degradation products of the high-molecular-weight LYDEX, and G2500PW_{XL} was used to examine oligomers, smaller monosaccharides, and amino acids, which were the higher-degradation products. GPC measurement conditions were as follows: mobile phase, 0.9% NaCl; flow rate, 0.6 mL/min; column temperature, 35 °C. Pullulan (STANDARD P-82, Showa Denko, Tokyo, Japan) was used as the reference standard.

3. Results and discussion

3-1. AD and SAPL characterization

Dextran was oxidized using sodium periodate. The reagents were added in predetermined amounts to establish an oxidant:dextran ratio of 2.5/20 (w/w). The aldehyde content of the produced AD was determined using iodine titration. The desired product was obtained, with an aldehyde content of 0.28 mol/AGU.

Several of the amino groups of ε-PLL were acylated with SA. The reagents were added in predetermined amounts to establish a reaction rate of 10 ± 5 mol%. According to ninhydrin measurement, the desired product was obtained, with an SA reaction rate of 12 mol%. These results are consistent with those of previous studies (Hyon et al., 2014; Matsumura et al., 2014), and these parameters were utilized in this study because polymers with these parameters showed good degradabilities and low cytotoxicities.

3-2. Degradation product analysis using GPC and gel degradation over time

The degradation of the LYDEX gel in physiological saline was analyzed using GPC. Figure 2 shows the gel degradation with time. The gel degrades rapidly on the first day of degradation to 35% residual, and degradation slows thereafter. The residual is 15% after 4 wk. The gel is not visually confirmed after 5 d.

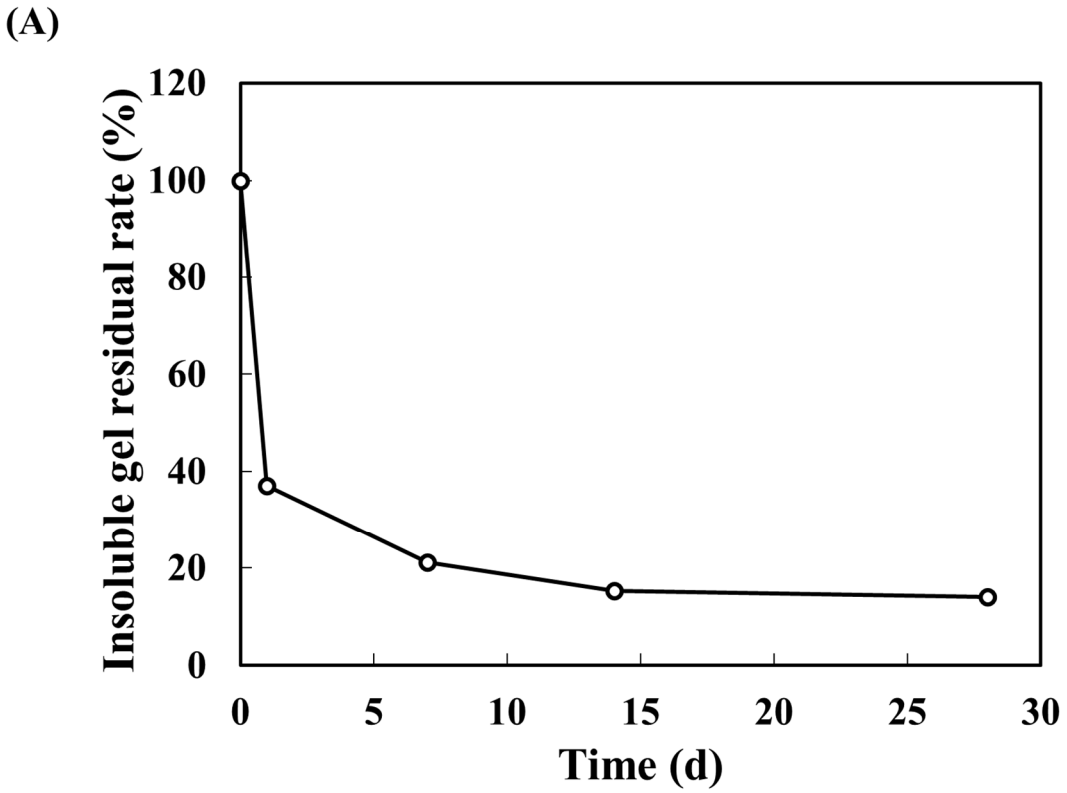

(B)

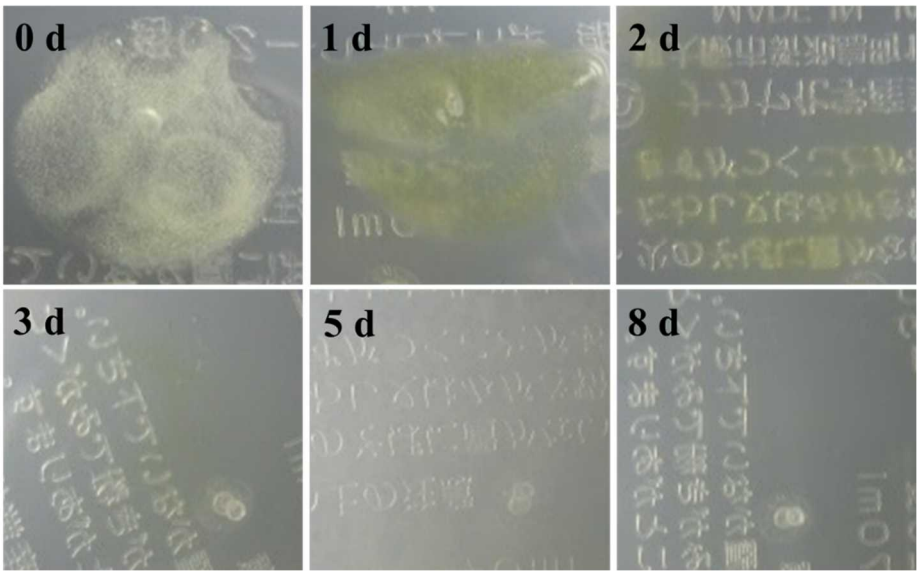

Figure 2. (A) Residual rate of LYDEX gel over time, (B) Degradation of LYDEX gel at 0, 1, 2, 3, 5, and 8 d at 37 °C in saline solution.

The absorption spectra of the filtrates of SAPL, AD, and LYDEX after 1 d of degradation are shown in Figure 3. A 210 nm absorption peak is observed for SAPL, whereas AD shows almost no absorption, with only a slight absorption maximum at approximately 240 nm. The 240 nm peak is due to a pH-dependent enol (Drobchenko et al., 1993). In addition, LYDEX immediately after gelation shows absorption only at 210 nm. Conversely, the LYDEX gel after 1 d of degradation shows absorption at approximately 210 and 323 nm. It gradually turns yellow due to the Maillard reaction (Chimpibul et al., 2016; Matsumura et al., 2014), and 323 nm is the absorption of this yellowing. Therefore, we conducted UV detection following GPC at 210 and 323 nm.

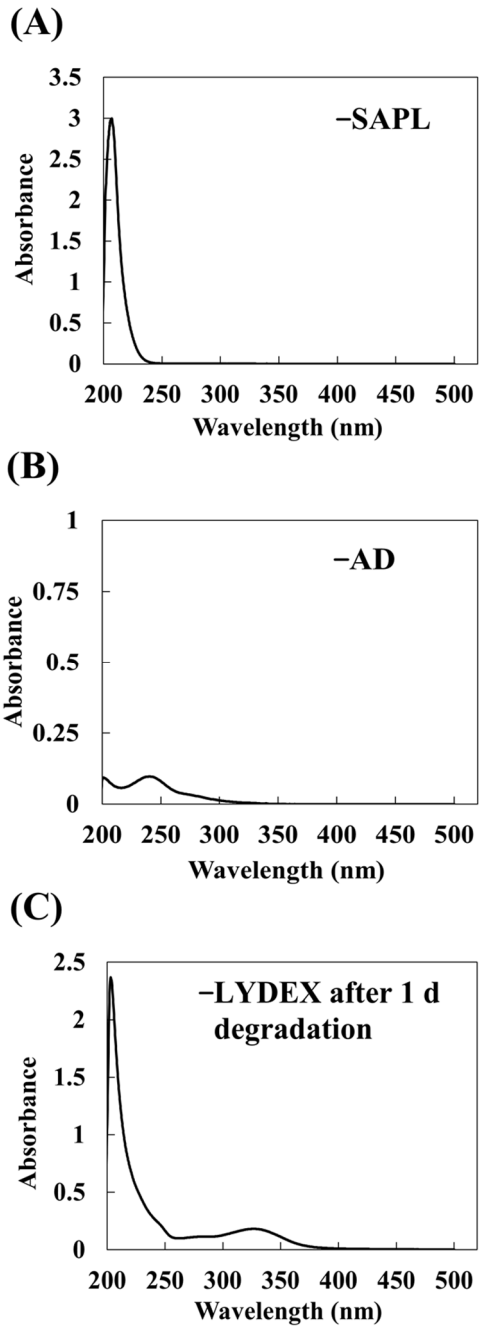

Figure 3. Absorption spectra of SAPL, AD, and the LYDEX gel degradation products.

The GPC chromatograms detected using refractive index (RI) detection are shown in Figure 4A. There is a small peak at a retention time (RT) of 10.4 min (Mw = more than several million grams per mole), a peak at 12.5 min RT (Mw = 145 900 g/mol), a large peak at 17.0 min RT (Mw = 11 200 g/mol), and a sharp peak at 19.6 min RT (Mw ≤ 2300 g/mol). All peak areas increase with time. For UV detection following GPC at 323 (Figure 4B) and 210 nm (Figure 4C), the peaks at 10.4, 12.5, and 17.0 min RT are observed at both wavelengths, but not the peak at 19.6 min RT. The peak at

10.4 min RT represents degradation products of Mw = more than several million grams per mole that are not separated by the TSKgel G4000PW$_{XL}$ column and appear in the exclusion limit. However, the peak at 17.0 min RT is much broader than that at 10.4 min RT, and as shown in Figure 2, LYDEX gel degrades rapidly and then slowly, suggesting that the degradation of LYDEX gel occurs as soon as the gel collapses and solubilizes, up to the Mw peak at 17.0 min RT (Mw = 11 200 g/mol). Meanwhile, there is an increase in the peak at 19.6 min RT (Mw ≤ 2300 g/mol) with time, and the fraction represented by this peak exhibits no UV absorption, suggesting that the compositions of the fractions with RTs of 19.6 and 17.0 min are different. The Mws of the degradation products are not uniformly distributed, and after 17.0 min RT, no degradation products with Mw = 3000 g/mol are observed up to RT 19.6 min (Mw ≤ 2300 g/mol).

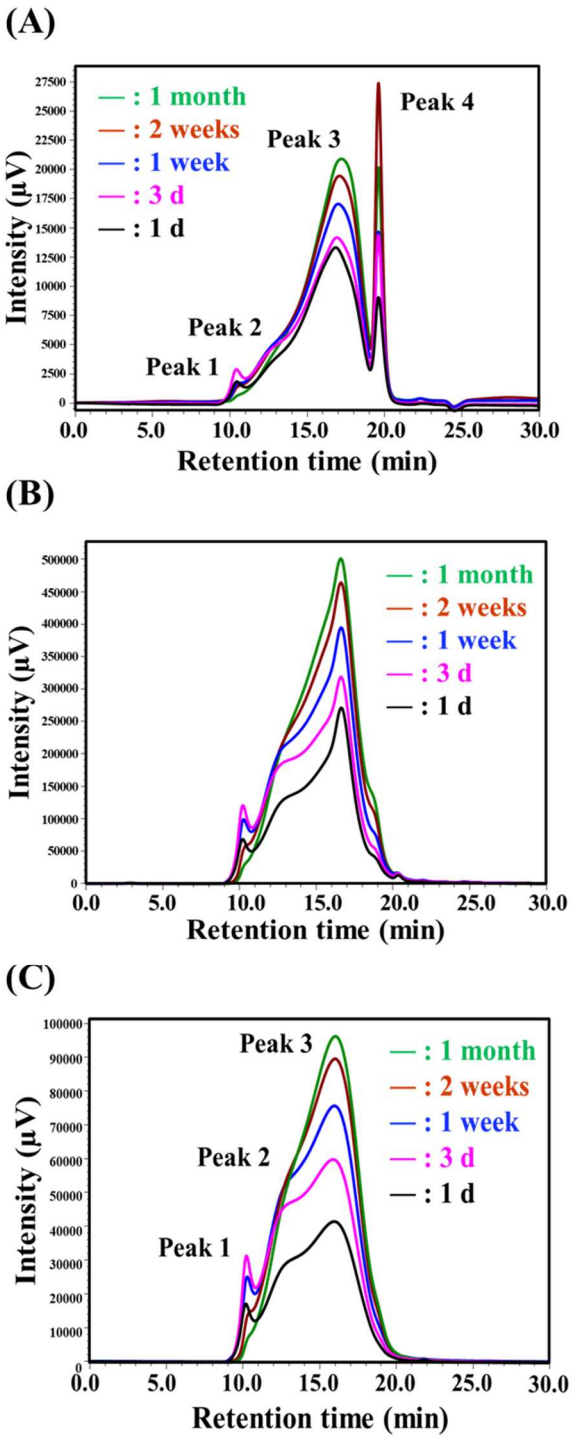

Figure 4. Gel permeation chromatograms obtained using G4000PW$_{XL}$ columns, of the products within the LYDEX degradation treatment solution; (A) refractive index detection, (B) ultraviolet (UV) detection at 323 nm, (C) UV detection at 210 nm.

3-3. GPC detection value ratio of each component

To observe the change in the formation behaviors of the LYDEX degradation products over time, the ratios of the three GPC detection values of LYDEX gel are compared with those of the raw materials AD and SAPL (Table 1). Differential refractometry of AD shows a single peak at 15.9 min RT (Mw = 73 000 g/mol, Figure S2), but almost no UV absorption is observed at 323 and 210 nm. AD is a polysaccharide, despite aldehyde group introduction, and the Mw of the starting material, dextran, is 70 000 g/mol, and hence these results are reasonable. The RI of SAPL (Figure S3) displays bimodal peaks at 17.3 (Mw = 11 000 g/mol) and 18.5 min RT (Mw = 3800 g/mol), in addition to UV absorption at 210 nm (Table 1). At 323 nm, very small bimodal peaks are observed. GPC was performed in the same manner for ε-PLL without the introduction of carboxyl groups (COOH 0% PLL) and polylysine with an increased carboxylation rate of 65% (COOH 65% PLL). The chromatograms reveal single peaks at 18.3 min RT (Mw = 4300 g/mol) for COOH 0% PLL and 16.9 min RT (Mw = 12 000 g/mol) for COOH 65% PLL. COOH 65% PLL is used as a cryoprotectant for cells (Matsumura & Hyon, 2009). ε-PLL is a polyamino acid consisting of 25–35 lysine amino acids that are ε-linked. SAPL is prepared by carboxylating 10% of these amino groups using SA. In COOH 65% PLL, 65% of the amino groups are carboxylated by increasing the amount of SA in the reaction. In COOH 65% PLL, the amino and carboxyl groups form aggregates via ionic bonding, and the Mw suggests that it is a trimer. In SAPL, 10% of the amino groups are carboxylated to form approximately 1/3 of the aggregate; thus, it exhibits bimodal peaks. For the

Table 1. Gel permeation chromatography detection value ratios of aldehyde-functionalized dextran (AD), succinic anhydride-treated poly-L-lysine (SAPL), and LYDEX against refractive index (RI) intensity.

		RI detection	*Ultraviolet (UV, 323 nm)*	*UV (210 nm)*
AD		1	0.0	0.2
SAPL (front peak)		1	0.1	70
Gel degradation peak	RT 10.4 min	1	13	54
	RT 12.5 min	1	13	54
	RT 17.0 min	1	4	21
	RT 19.6 min	1	0.0	2

RT, retention time.

The peak area of each component is expressed as a relative value when the RI value is set to 1, calculated using UV intensity / RI intensity (unit: mv).

degradation products of LYDEX gel, detection of the small peaks at 10.4 min RT using UV at 323 and 210 nm is more sensitive than RI detection. Even at 17.0 min RT, UV is more sensitive than RI, but less sensitive than UV at 10.4 min RT. At 19.6 min RT, no UV absorption is observed at 323 nm, and even at 210 nm, the sensitivity is lower than that at 10.4- and 17.0-min RT.

Comparing AD and SAPL, only the degradation product of LYDEX gel exhibits UV absorption at 323 nm, suggesting that UV absorption occurs following the Maillard reaction of the Schiff base. As there is no UV absorption at 323 nm at 19.6 min RT, there is therefore no Maillard reaction component from the imine bond (Schiff base) in the fraction represented by this peak. In addition, because the Mw of SAPL is 4000 g/mol, the degradation product is an oligodextran structure, similar to a degradation product of AD undergoing the Maillard reaction. Although the initial reaction pathway of the Maillard reaction is long known (Hayashi & Namiki, 1986; Hodge, 1953), the Schiff bases are isomerized via Amadori rearrangement to ketoamines, which are likely connected to the side chains of SAPL.

3-4. Temporal behaviors of main degradation products

To evaluate the temporal changes in the small-molecule products within the LYDEX gel degradation treatment solution, GPC was performed using a TSKgel G2500PW$_{XL}$ column (Figure 5).

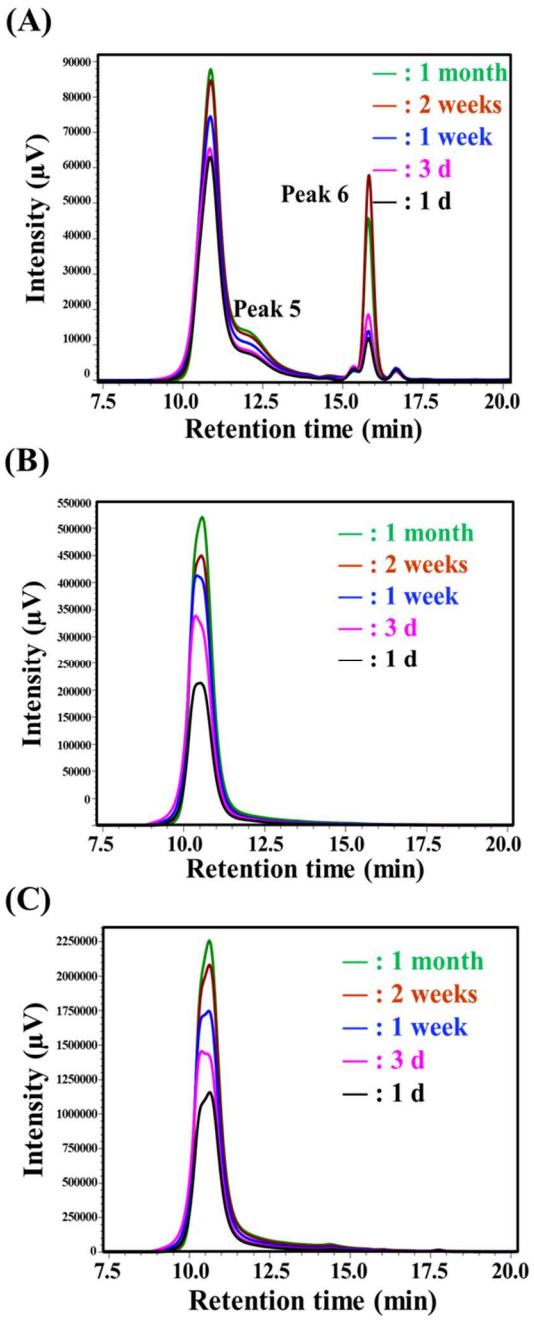

Figure 5. Gel permeation chromatography, using a G2500PW$_{XL}$ column, of the products within LYDEX degradation treatment solution; (A) refractive index detection, (B) ultraviolet (UV) detection at 323 nm, (C) UV detection at 210 nm.

Using the TSKgel G2500PW$_{XL}$ column, peaks 5 and 6 at 12.2- and 15.8-min RT, respectively, are the characteristic peaks, in addition to the peak at 10.7 min RT that elutes near the exclusion limit of the column. Of these peaks, 4 and 6 are consistent with the RT of NaCl, and their irregularities,

rather than changes over time, suggest that NaCl and low-molecular-weight compounds may elute together.

Figure 6 shows the changes in the RI signals of peaks 1, 2, 3, and 5 with increasing degradation time, as shown in Figures 4 and 5. Peak 1 increases initially, but then slowly decreases. The trends of peaks 3 and 5 are similar, with slight increases even after 1 mo. The trend of peak 2 is similar to that of peak 1, increasing initially and remaining constant for a while, but then gradually decreasing. The Mw distribution values for each peak show no significant changes, suggesting the formation of a metastable substance over time (Table S1). First, peak 1 represents macromolecules with Mws of >1 million grams per mole, which initially form and then gradually degrade when dissolved. Peak 2 represents compounds with Mws of several hundred thousand grams per mole, and their formation, due to the degradation of the gel and compounds represented by peak 1, and their degradation in the dissolved state occur in parallel, gradually decreasing over time. In addition, peak 3 represents compounds with Mws of 10 000–20 000 g/mol, and peak 5 represents compounds with Mws of several thousand, but they are constantly increasing with the convergence to the formation of these compounds during the final stage of degradation.

Figure S4 shows the GP chromatogram of the degradation treatment solution (1 wk), obtained using a TSKgel G2500PW$_{XL}$ column. A large peak (10.8 min RT) is observed in the exclusion limit of the column, followed by a gentle peak to a shoulder centered at 11.8 min RT (Mw = 2500 g/mol) and peaks at 14.4, 15.3, 15.8, 16.6, and 17.2 min RT. The fractions below Mw = 2500 g/mol show almost no UV absorption at 323 and 210 nm and represent degradation products of the oligodextran moiety

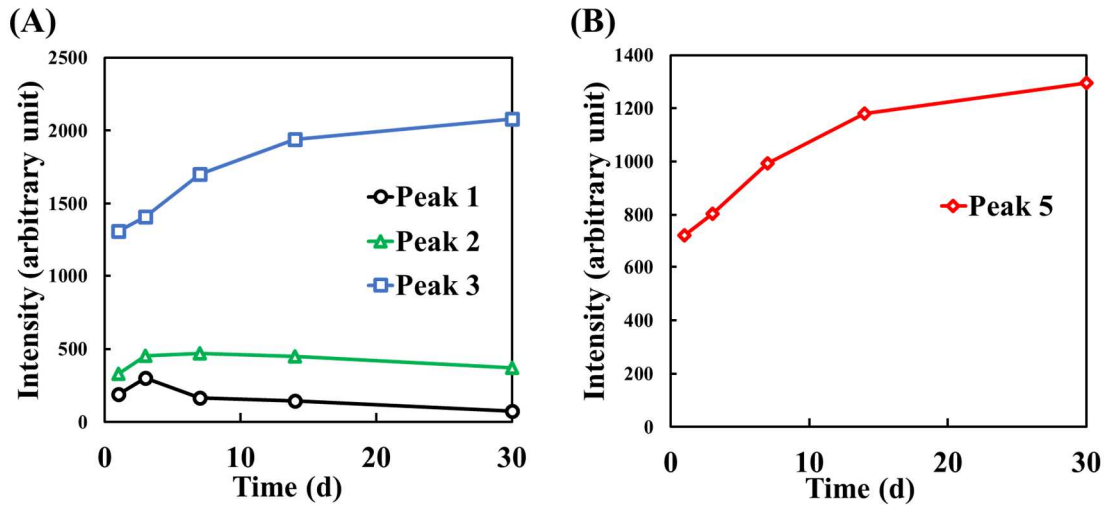

Figure 6. Changes in the degradation products (main peaks) over time in the degradation treatment solution; (A) Refractive index (RI) detection following elution from the G4000PW$_{XL}$ column and (B) RI detection following elution from the G2500PW$_{XL}$ column.

generated by degradation, because no Schiff base (C=N bond) is present, as described above. Glucose reacts with proteins to produce glyoxal (Wells-Knecht et al., 1995) (Mw = 58.04 g/mol), which is formed by autoxidation of glucose undergoing the Maillard reaction, glycolaldehyde (Glomb & Monnier, 1995) (Mw = 254.39 g/mol), which is derived from Schiff bases, and methylglyoxal (Thornalley, 1993) (Mw = 72.06 g/mol), 3-deoxyglucosone (Kato et al., 1989) (Mw = 162.14 g/mol), and glucosone (Kawakishi et al., 1990) (Mw = 178.140 g/mol), which are formed by the Schiff base and degradation of Amadori rearrangement products. Therefore, AD-derived Amadori rearrangement products and their degradation products, which are smaller than glucose, suggested to be emerging.

3-5. IR spectroscopy

The IR spectra of the samples that showed the major peaks after preparative isolation using GPC, dialysis, lyophilization, and concentration are shown in Figure 7. For comparison, AD and SAPL, which are components of LYDEX, were also measured in the same manner. AD exhibits no aldehyde group absorption (~1700 cm^{-1}), instead showing strong ether bond absorption, suggesting that the aldehyde group is converted to a hemiacetal (ether bond) via reaction with water, which is the characteristic absorption. The lack of aldehyde group absorption is consistent with the study by Maia et al. (Maia et al., 2005) and its absence for iodate-oxidized polysaccharides is generally due to the formation of gem-diol with hydrated hemiacetal groups (Sloan et al., 1954).

The characteristic IR signals of amides are amide I (1600–1800 cm^{-1}), amide II (1470–1570 cm^{-1}), amide III (1250–1350 cm^{-1}), and amide A (3300–3500 cm^{-1}). SAPL is characterized by strong absorption, particularly at approximately 3400 and 1620 cm^{-1} due to the amide group, which are consistent with the reported signals of PLL (De Campos Vidal & Mello, 2011). The spectrum of the compounds represented by preparative peak 1 shows the characteristic absorptions reflecting the structures of AD and SAPL. For the compounds represented by preparative peak 2, similar to peak 1, the peaks reflecting the structures of AD and SAPL are observed, but the amide II band of SAPL at approximately 1500 cm^{-1} is completely absent, and the ether absorption increased slightly, suggesting that the AD component increased relative to that of the fraction represented by peak 1. For the compounds represented by preparative peak 3, the absorption of amide reduced and the absorption of ether, which reflects the structure of AD, is observed, thereby rendering the spectrum even closer to that of AD than that of peak 2.

For the compounds represented by preparative peak 5, as for preparative peak 3, absorption reflecting the structure of AD is strong, and the spectrum is close to that of AD, but the amide absorption due to SAPL (~1620 cm^{-1}) is also observed. In summary, the spectrum of the compounds represented by preparative peak 1 is close to that of SAPL, the spectra of the compounds represented

by preparative peaks 3 and 5 are close to that of AD, and the compounds represented by preparative

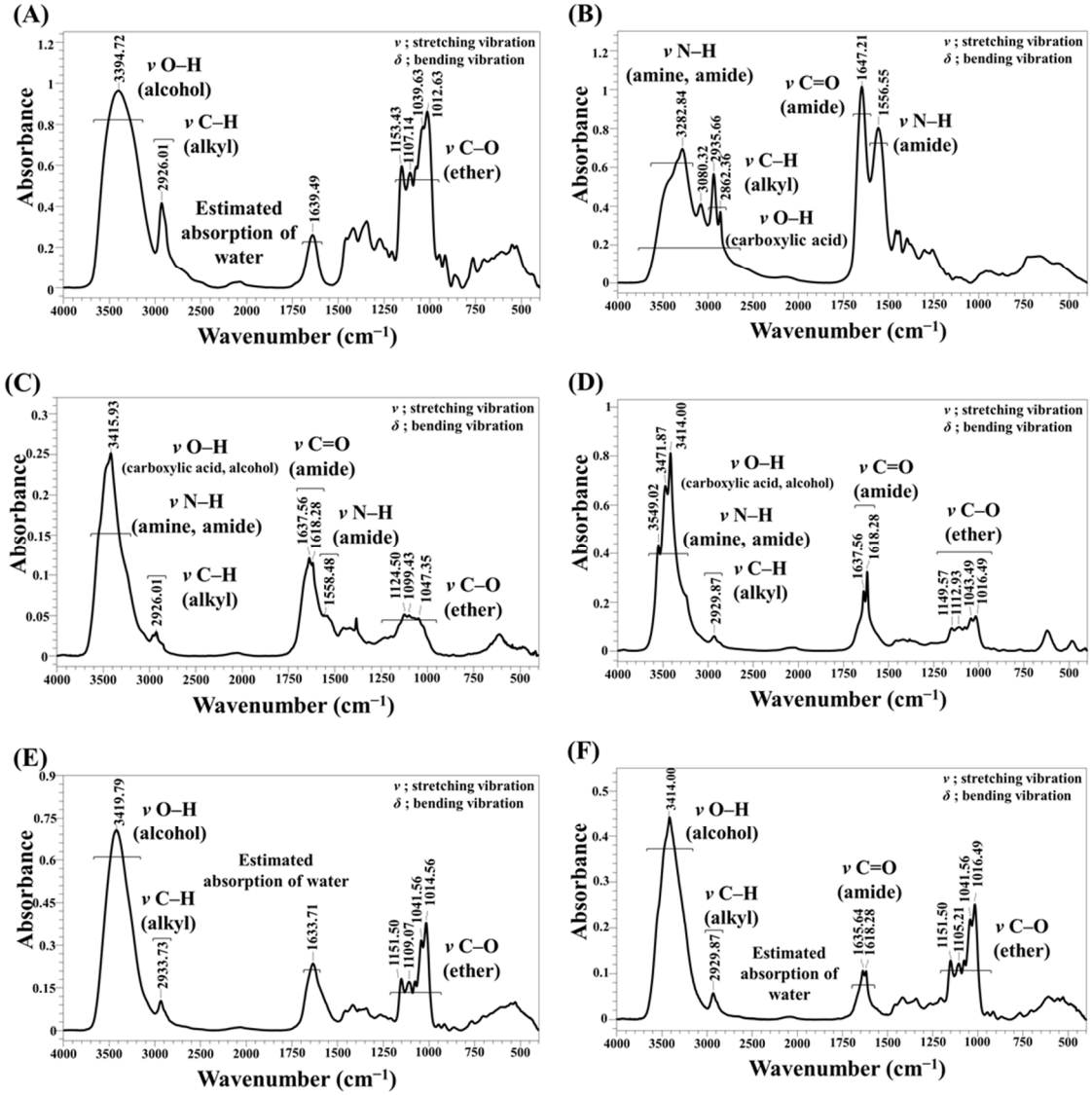

Figure 7. (A) Infrared (IR) spectrum of AD. (B) IR spectrum of SAPL. (C) IR spectrum of the fraction represented by preparative peak 1, (D) peak 2, (E) peak 3, and (F) peak 5.

peak 2 include AD and SAPL. Therefore, as the preparative peak shifts from 1 to 2 to 3 and 5 to the low-molecular-weight region, the structure shifts from relatively rich in the SAPL skeleton to rich in the AD skeleton. This refers not only to the whole structure but also to the substructure.

3-6. NMR spectroscopy

The ^{1}H NMR spectra of the preparative samples represented by peaks 2, 3, and 5 are shown in Figure 8. For comparison, AD and SAPL, the raw materials of LYDEX, were also measured in the

same manner. Preparative peak 1 was not analyzed due to insufficient sensitivity for the small

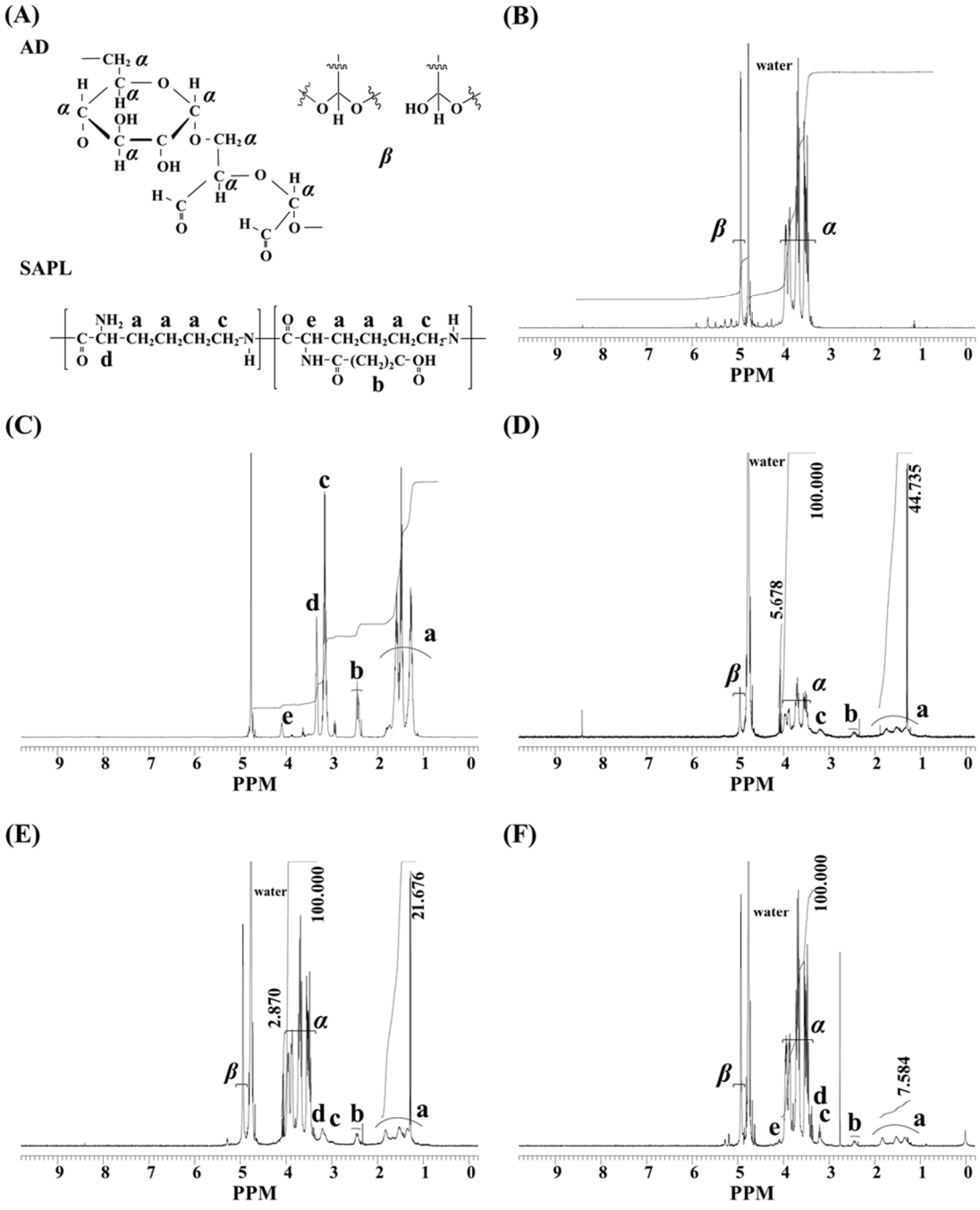

Figure 8. (A) Chemical structures of AD and SAPL. (B) ^{1}H NMR spectrum of AD. (C) ^{1}H NMR spectrum of SAPL. (D) ^{1}H NMR spectrum of the compounds represented by preparative peak 2, (E) peak 3, and (F) peak 5.

amount within the preparative volume. AD is characterized by methine and methylene signals representing protons adjacent to O atoms on the dextran backbone (α in the figure) and signals

representing protons between hemiacetals (or acetals) (β in the figure). There are no signals attributed to the aldehyde protons. The C2–C3 and C3–C4 bonds of the glucose moiety are removed by oxidation, suggesting that C2 and C4, which are replaced by aldehydes, react with hydroxyl groups and are converted to the hemiacetal structure (ether bond) (Aalmo et al., 1981; Ishak & Painter, 1978; Yu & Bishop, 1967).

SAPL is characterized by signals such as those representing the adjacent methylene on the PLL backbone (a), the methylene adjacent to the carbonyl group on the succinate backbone (b), the methylene adjacent to the imine (c), and the proton on the C atom to which the amino group is attached (d). There are signals attributed to the α proton (e). Matsumura et al. reported the similar structural properties of succinylated PLLs at different carboxylation rates (Matsumura et al., 2013), although the carboxylation rate of SAPL is different from those reported previously.

The compounds represented by the preparative peaks 2, 3, and 5 exhibit the characteristic peaks (α, β, a, b, c, and d) of AD and SAPL in all samples, suggesting that the structure is a hybrid of these skeletons. However, the structures of the degradation products represented by each preparative peak appear to shift from SAPL to AD skeleton-rich from preparative fraction 2 to 3 to 5 to the low molecular weight region, which is consistent with the IR spectra. The methine/methylene group increases from preparative fractions 2 to 3. Figures 7(D) and (E) show that the AD-derived peaks increase as the degradation of LYDEX progresses. The progress of the Maillard reaction deduced using previous studies (Chimpibul et al., 2016) (Figure S1(A)) and the methylene group as one of the components of 3-deoxyosone that undergoes Strecker degradation via Amadori rearrangement (Tressl et al., 1995) suggest that these peaks are due to an AD-derived degradation product. Conversely, as SAPL is stable in water and AD undergoes the Maillard reaction, alteration of the SAPL structure is unlikely, and the SAPL-derived methine/methylene group is observed. Thus, this increase suggests that the degradations of AD and SAPL are related to the Maillard reaction.

For preparative fractions 2, 3, and 5, the peak integrals of the glucose-derived signals of AD observed at 3.3–4.0 ppm are set to 100, and the peak integrals of the methylene-derived signals of SAPL observed at 1.2–1.9 ppm are compared. The SAPL/AD ratio is 4:2:1 for the preparative fractions 2:3:5.

Therefore, after AD and SAPL form a Schiff base, the main chain of AD is broken via Amadori rearrangement and molecular degradation commences, with AD degrading into Amadori rearrangement products and their degradation products; in addition, the Schiff bases of AD and SAPL are loosely bound via C–N, but SAPL retains most of the PLL structure, and as PLL is stable in aqueous solution (Hiraki, 1995), SAPL remains bound to a section of AD. This AD-bound SAPL becomes a polymer with an Mw of approximately 4000–5000 g/mol, which forms dimeric or trimeric aggregates, remaining undegraded.

4. Conclusions

To elucidate the degradation mechanism of LYDEX in aqueous media, the main degradation products were analyzed, and the following degradation mechanisms were clarified. The analysis of degradation products using GPC showed that LYDEX became >60% water-soluble in 1 d, with mild subsequent solubilization. Degradation product analysis using GPC, followed by IR and ^{1}H NMR spectroscopy, revealed products with mixed structures containing SAPL and AD moieties. According to the IR and ^{1}H NMR spectra, the later the GPC elution, the higher the percentage of the AD moieties, and in the fractions 2, 3, and 5 collected in this study, the SAPL/AD ratio changed from approximately 4 to 2 to 1, respectively, based on the ^{1}H NMR peak integrals. The methylene group increased from fraction 2 to 3 and was one of the components of 3-deoxyosone that underwent Strecker degradation via Amadori rearrangement, suggesting that it was related to the Maillard reaction.

The mixture of AD and SAPL became richer in AD as the Mw decreased. After the main chains of the solubilized degradation products of LYDEX were cleaved via Amadori rearrangement (Figure S1(B)), the structure of the AD-SAPL network, with Mws from several million to 145 000 g/mol, was potentially maintained for a while, wherein the SAPL skeleton remained undegraded and the AD portion degraded to oligodextran, with an Mw of > 2300 g/mol. However, the low-molecular-weight fractions of peaks 4 and 6 were not included in this analytical study because of irregular fluctuations that suggested potential contamination by NaCl or other substances. Specifically, peaks 4 and 6 increased with processing time, in addition to other degradation peaks in the GP chromatograms, as shown in Figure 6. In addition, the RTs of these peaks are consistent with that of NaCl and may therefore simply represent NaCl or organic compounds, such as sugars (alone), generated by LYDEX degradation.

Although LYDEX gel should not degrade further in saline solution, the *in vivo* degradation and absorption mechanism should be clarified in combination with data from *in vivo* kinetics and implantation studies for clinical application.

Macromolecules, such as polyvinylpyrrolidone and albumin, enter cells via endocytosis (Silverstein et al., 1977), and these macromolecules undergo digestion by endosomes formed there, which fuse with lysosomes. A Schiff base-bound Adriamycin-oxidized dextran (using a 70 kDa dextran) complex was used to study the intracellular form of Adriamycin, speculating that it is absorbed into tissue cells via endocytosis and then undergoes low-molecular-weight conversion by lysosomes (Munechika et al., 1994).

This suggests that, similar to LYDEX, degradation products formed via gel microfragmentation due to self-degradation and high-molecular-weight degradation products are likely digested *in vivo* through phagocytosis by phagocytes, such as macrophages, absorbed into the spleen and liver, and

degraded to low molecular weight via metabolism *in vivo*. When LYDEX gels are applied in the gastrointestinal tract, such as endoscopic wound dressings, AD and AD-derived degradation products may be reduced by enzymes to sugars, such as dextranase and isomaltose, several of which are utilized in the metabolic cycle *in vivo*, and several are eliminated. Regarding the pharmacokinetics of SAPL and SAPL-derived degradation products, low absorption of ^{14}C-radiolabeled ε-PLL in the gastrointestinal tract was observed in an absorption, distribution, metabolism, and excretion (ADME) study using oral administration (Hiraki et al., 2003), and SAPL and SAPL-derived degradation products may therefore pass through the fecal gastrointestinal tract without absorption. Finally, hydrogels obtained by the reaction of AD with polymers bearing amino groups, such as collagen, have been previously reported. However, the *in vitro* degradation behavior of LYDEX by the reaction of AD with SAPL, as shown in this study, revealed LYDEX self-degradability for the first time. This is extremely valuable for the study of molecular degradation mechanisms of polysaccharide hydrogels and the development of medical applications, such as hemostatic agents, sealants, and anti-adhesion materials.

Acknowledgments

The authors thank Toray Research Center, Inc. for their assistance with IR and ^{1}H NMR spectroscopy.

Funding sources

This research did not receive any specific grant from funding agencies in the public, commercial, or not-for-profit sectors.

Conflict of interest

Woogi Hyon and Suong-Hyu Hyon are founders of BMG, Inc.

Shuji Shibata, Etsuo Ozaki, and Motoki Fujimura are employees of BMG, Inc.

References

Aalmo, K. M., Grasdalen, H., Painter, T. J., & Krane, J. (1981). Characterisation by 1H- and 13C-n.m.r. spectroscopy of the products from oxidation of methyl α- and β-d-galactopyranoside with periodic acid in dimethyl sulphoxide. *Carbohydrate Research*, *91*(1), 1–11. https://doi.org/10.1016/S0008-6215(00)80985-4

Araki, M., Tao, H., Nakajima, N., Sugai, H., Sato, T., Hyon, S. H., Nagayasu, T., & Nakamura, T. (2007). Development of new biodegradable hydrogel glue for preventing alveolar air leakage.

Journal of Thoracic and Cardiovascular Surgery, *134*(5), 1241–1248. https://doi.org/10.1016/j.jtcvs.2007.07.020

Araki, M., Tao, H., Sato, T., Nakajima, N., Sugai, H., Hyon, S. H., Nagayasu, T., & Nakamura, T. (2007). Creation of a uniform pleural defect model for the study of lung sealants. *Journal of Thoracic and Cardiovascular Surgery*, *134*(1), 145–151. https://doi.org/10.1016/j.jtcvs.2007.01.007

Bang, B. W., Lee, E., Maeng, J. H., Kim, K., Hwang, J. H., Hyon, S. H., Hyon, W., & Lee, D. H. (2019). Efficacy of a novel endoscopically deliverable muco-adhesive hemostatic powder in an acute gastric bleeding porcine model. *PLoS ONE*, *14*(6), e0216829. https://doi.org/10.1371/journal.pone.0216829

Bhatia, S. K., Arthur, S. D., Chenault, H. K., & Kodokian, G. K. (2007). Interactions of polysaccharide-based tissue adhesives with clinically relevant fibroblast and macrophage cell lines. *Biotechnology Letters*, *29*(11), 1645–1649. https://doi.org/10.1007/s10529-007-9465-8

Cadée, J. A., Van Luyn, M. J. A., Brouwer, L. A., Plantinga, J. A., Van Wachem, P. B., De Groot, C. J., Den Otter, W., & Hennink, W. E. (2000). In vivo biocompatibility of dextran-based hydrogels. *Journal of Biomedical Materials Research*, *50*(3), 397–404.

Canonico, S. (2003). The use of Human Fibrin Glue in the surgical operations. *Acta Biomedica de l'Ateneo Parmense*, *74*(SUPPL. 2), 21–25. https://pubmed.ncbi.nlm.nih.gov/15055028/

Chao, H. H., & Torchiana, D. F. (2003). BioGlue: Albumin/Glutaraldehyde Sealant in Cardiac Surgery. *Journal of Cardiac Surgery*, *18*(6), 500–503. https://doi.org/10.1046/j.0886-0440.2003.00304.x

Chimpibul, W., Nagashima, T., Hayashi, F., Nakajima, N., Hyon, S. H., & Matsumura, K. (2016). Dextran oxidized by a malaprade reaction shows main chain scission through a maillard reaction triggered by schiff base formation between aldehydes and amines. *Journal of Polymer Science, Part A: Polymer Chemistry*, *54*(14), 2254–2260. https://doi.org/10.1002/pola.28099

Chimpibul, W., Nakaji-Hirabayashi, T., Yuan, X., & Matsumura, K. (2020). Controlling the degradation of cellulose scaffolds with Malaprade oxidation for tissue engineering. *Journal of Materials Chemistry B*, *8*(35), 7904–7913. https://doi.org/10.1039/d0tb01015d

559 De Campos Vidal, B., & Mello, M. L. S. (2011). Collagen type I amide I
560 band infrared spectroscopy. *Micron*, *42*(3), 283–289.
561 https://doi.org/10.1016/j.micron.2010.09.010
562 Drobchenko, S. N., Isaeva-Ivanova, L. S., Kleiner, A. R., Lomakin, A. V.,
563 Kolker, A. R., & Noskin, V. A. (1993). An investigation of the
564 structure of periodate-oxidised dextran. *Carbohydrate Research*,
565 *241*(C), 189–199. https://doi.org/10.1016/0008-6215(93)80105-N
566 Drury, J. L., & Mooney, D. J. (2003). Hydrogels for tissue engineering:
567 Scaffold design variables and applications. In *Biomaterials* (Vol. 24,
568 Issue 24, pp. 4337–4351). Elsevier BV. https://doi.org/10.1016/S0142-
569 9612(03)00340-5
570 Elvin, C. M., Danon, S. J., Brownlee, A. G., White, J. F., Hickey, M.,
571 Liyou, N. E., Edwards, G. A., Ramshaw, J. A. M., & Werkmeister, J.
572 A. (2010). Evaluation of photo-crosslinked fibrinogen as a rapid and
573 strong tissue adhesive. *Journal of Biomedical Materials Research -*
574 *Part A*, *93*(2), 687–695. https://doi.org/10.1002/jbm.a.32572
575 Elvin, Christopher M., Brownlee, A. G., Huson, M. G., Tebb, T. A., Kim,
576 M., Lyons, R. E., Vuocolo, T., Liyou, N. E., Hughes, T. C., Ramshaw,
577 J. A. M., & Werkmeister, J. A. (2009). The development of
578 photochemically crosslinked native fibrinogen as a rapidly formed and
579 mechanically strong surgical tissue sealant. *Biomaterials*, *30*(11),
580 2059–2065. https://doi.org/10.1016/j.biomaterials.2008.12.059
581 Elvin, Christopher M., Vuocolo, T., Brownlee, A. G., Sando, L., Huson, M.
582 G., Liyou, N. E., Stockwell, P. R., Lyons, R. E., Kim, M., Edwards, G.
583 A., Johnson, G., McFarland, G. A., Ramshaw, J. A. M., &
584 Werkmeister, J. A. (2010). A highly elastic tissue sealant based on
585 photopolymerised gelatin. *Biomaterials*, *31*(32), 8323–8331.
586 https://doi.org/10.1016/j.biomaterials.2010.07.032
587 Erasmi, A. W., Sievers, H. H., Wohlschläger, C., Hewitt, C. W., Marra, S.
588 W., Kann, B. R., Tran, H. S., Puc, M. M., Chrzanowski, F. A., Tran, J.
589 L. V., Cilley, J. H., Simonetti, V. A., DelRossi, A. J., & Lenz, S. D.
590 (2002). Inflammatory response after BioGlue application [6] (multiple
591 letters). In *Annals of Thoracic Surgery* (Vol. 73, Issue 3, pp. 1025–
592 1026). Elsevier Inc. https://doi.org/10.1016/s0003-4975(01)03524-x
593 Fancy, D. A., & Kodadek, T. (1999). Chemistry for the analysis of protein-
594 protein interactions: Rapid and efficient cross-linking triggered by long

595 wavelength light. *Proceedings of the National Academy of Sciences of*
596 *the United States of America*, *96*(11), 6020–6024.
597 https://doi.org/10.1073/pnas.96.11.6020
598 Ferreira, L., Rafael, A., Lamghari, M., Barbosa, M. A., Gil, M. H., Cabrita,
599 A. M. S., & Dordick, J. S. (2004). Biocompatibility of
600 chemoenzymatically derived dextran-acrylate hydrogels. *Journal of*
601 *Biomedical Materials Research - Part A*, *68*(3), 584–596.
602 https://doi.org/10.1002/jbm.a.20102
603 Fuller, C. (2013). Reduction of intraoperative air leaks with Progel in
604 pulmonary resection: A comprehensive review. In *Journal of*
605 *Cardiothoracic Surgery* (Vol. 8, Issue 1, pp. 1–7). BioMed Central.
606 https://doi.org/10.1186/1749-8090-8-90
607 Fürst, W., & Banerjee, A. (2005). Release of glutaraldehyde from an
608 albumin-glutaraldehyde tissue adhesive causes significant in vitro and
609 in vivo toxicity. *Annals of Thoracic Surgery*, *79*(5), 1522–1528.
610 https://doi.org/10.1016/j.athoracsur.2004.11.054
611 Gilbert, T. W., Badylak, S. F., Gusenoff, J., Beckman, E. J., Clower, D. M.,
612 Daly, P., & Rubin, J. P. (2008). Lysine-derived urethane surgical
613 adhesive prevents seroma formation in a canine abdominoplasty
614 model. *Plastic and Reconstructive Surgery*, *122*(1), 95–102.
615 https://doi.org/10.1097/PRS.0b013e31817743b8
616 Glomb, M. A., & Monnier, V. M. (1995). Mechanism of protein
617 modification by glyoxal and glycolaldehyde, reactive intermediates of
618 the Maillard reaction. *Journal of Biological Chemistry*, *270*(17),
619 10017–10026. https://doi.org/10.1074/jbc.270.17.10017
620 Hayashi, T., & Namiki, M. (1986). Role of sugar fragmentation in an early
621 stage browning of amino-carbonyl reaction of sugar with amino acid.
622 *Agricultural and Biological Chemistry*, *50*(8), 1965–1970.
623 https://doi.org/10.1080/00021369.1986.10867692
624 Hill, A., Estridge, T. D., Maroney, M., Monnet, E., Egbert, B., Cruise, G.,
625 & Coker, G. T. (2001). Treatment of suture line bleeding with a novel
626 synthetic surgical sealant in a canine iliac PTFE graft model. *Journal*
627 *of Biomedical Materials Research*, *58*(3), 308–312.
628 Hino, M., Ishiko, O., Honda, K. I., Yamane, T., Ohta, K., Takubo, T., &
629 Tatsumi, N. (2000). Transmission of symptomatic parvovirus B19
630 infection by fibrin sealant used during surgery. *British Journal of*

Haematology, *108*(1), 194–195. https://doi.org/10.1046/j.1365-2141.2000.01818.x

Hiraki, J. (1995). Basic and applied studies on ε-polylysine. *Journal of Antibacterial and Antifungal Agents*, 23, 349-354.

Hiraki, J., Ichikawa, T., Ninomiya, S. I., Seki, H., Uohama, K., Seki, H., Kimura, S., Yanagimoto, Y., & Barnett, J. W. (2003). Use of ADME studies to confirm the safety of ε-polylysine as a preservative in food. *Regulatory Toxicology and Pharmacology*, *37*(2), 328–340. https://doi.org/10.1016/S0273-2300(03)00029-1

Hodge, J. E. (1953). Dehydrated foods, Chemistry of Browning Reactions in Model Systems. *Journal of Agricultural and Food Chemistry*, *1*(15), 928–943. https://doi.org/10.1021/jf60015a004

Hyon, S. H., Nakajima, N., Sugai, H., & Matsumura, K. (2014). Low cytotoxic tissue adhesive based on oxidized dextran and epsilon-poly- l -lysine. *Journal of Biomedical Materials Research - Part A*, *102*(8), 2511–2520. https://doi.org/10.1002/jbm.a.34923

Ishak, M. F., & Painter, T. J. (1978). Kinetic evidence for hemiacetal formation during the oxidation of dextran in aqueous periodate. *Carbohydrate Research*, *64*(C), 189–197. https://doi.org/10.1016/S0008-6215(00)83700-3

Ishihara, M., Nakanishi, K., Ono, K., Sato, M., Kikuchi, M., Saito, Y., Yura, H., Matsui, T., Hattori, H., Uenoyama, M., & Kurita, A. (2002). Photocrosslinkable chitosan as a dressing for wound occlusion and accelerator in healing process. *Biomaterials*, *23*(3), 833–840. https://doi.org/10.1016/S0142-9612(01)00189-2

Kamitani, T., Masumoto, H., Kotani, H., Ikeda, T., Hyon, S. H., & Sakata, R. (2013). Prevention of retrosternal adhesion by novel biocompatible glue derived from food additives. *Journal of Thoracic and Cardiovascular Surgery*, *146*(5), 1232–1238. https://doi.org/10.1016/j.jtcvs.2013.02.001

Kato, H., Hayase, F., Shin, D. B., Oimomi, M., & Baba, S. (1989). 3-Deoxyglucosone, an intermediate product of the Maillard reaction. *Progress in Clinical and Biological Research*, *304*, 69–84. https://europepmc.org/article/med/2780681

Kawakishi, S., Okawa, Y., & Uchida, K. (1990). Oxidative Damage of Protein Induced by the Amadori Compound-Copper Ion System.

Journal of Agricultural and Food Chemistry, *38*(1), 13–17. https://doi.org/10.1021/jf00091a003

Khalikova, E., Susi, P., & Korpela, T. (2005). Microbial Dextran-Hydrolyzing Enzymes: Fundamentals and Applications. *Microbiology and Molecular Biology Reviews*, *69*(2), 306–325. https://doi.org/10.1128/mmbr.69.2.306-325.2005

Kobayashi, H., Sekine, T., Nakamura, T., & Shimizu, Y. (2001). In vivo evaluation of a new sealant material on a rat lung air leak Model. *Journal of Biomedical Materials Research*, *58*(6), 658–665. https://doi.org/10.1002/jbm.1066

LeMaire, S. A., Schmittling, Z. C., Coselli, J. S., Ündar, A., Deady, B. A., Clubb, F. J., & Fraser, C. D. (2002). BioGlue surgical adhesive impairs aortic growth and causes anastomotic strictures. *Annals of Thoracic Surgery*, *73*(5), 1500–1506. https://doi.org/10.1016/S0003-4975(02)03512-9

Lévesque, S. G., & Shoichet, M. S. (2007). Synthesis of enzyme-degradable, peptide-cross-linked dextran hydrogels. *Bioconjugate Chemistry*, *18*(3), 874–885. https://doi.org/10.1021/bc0602127

Li, C., Wang, T., Hu, L., Wei, Y., Liu, J., Mu, X., Nie, J., & Yang, D. (2014). Photocrosslinkable bioadhesive based on dextran and PEG derivatives. *Materials Science and Engineering C*, *35*(1), 300–306. https://doi.org/10.1016/j.msec.2013.10.032

Liu, G., Shi, Z., Kuriger, T., Hanton, L. R., Simpson, J., Moratti, S. C., Robinson, B. H., Athanasiadis, T., Valentine, R., Wormald, P. J., & Robinson, S. (2009). Synthesis and characterization of chitosan/dextran-based hydrogels for surgical use. *Macromolecular Symposia*, *279*(1), 151–157. https://doi.org/10.1002/masy.200950523

MacGillivray, T. E. (2003). Fibrin Sealants and Glues. *Journal of Cardiac Surgery*, *18*(6), 480–485. https://doi.org/10.1046/j.0886-0440.2003.02073.x

Maia, J., Carvalho, R. A., Coelho, J. F. J., Simões, P. N., & Gil, M. H. (2011). Insight on the periodate oxidation of dextran and its structural vicissitudes. *Polymer*, *52*(2), 258–265. https://doi.org/10.1016/j.polymer.2010.11.058

Maia, J., Ferreira, L., Carvalho, R., Ramos, M. A., & Gil, M. H. (2005). Synthesis and characterization of new injectable and degradable

703 dextran-based hydrogels. *Polymer*, *46*(23), 9604–9614.
704 https://doi.org/10.1016/j.polymer.2005.07.089
705 Malaprade, L. (1928). Action of polyalcohols on periodic acid. Analytical
706 application. *Bulletin de La Societe Chimique de France*, *43*, 683–696.
707 Massia, S. P., & Stark, J. (2001). Immobilized RGD peptides on surface-
708 grafted dextran promote biospecific cell attachment. *Journal of*
709 *Biomedical Materials Research*, *56*(3), 390–399.
710 Matsumura, K., Hayashi, F., Nagashima, T., & Hyon, S. H. (2013). Long-
711 term cryopreservation of human mesenchymal stem cells using
712 carboxylated poly-l-lysine without the addition of proteins or dimethyl
713 sulfoxide. *Journal of Biomaterials Science, Polymer Edition*, *24*(12),
714 1484–1497. https://doi.org/10.1080/09205063.2013.771318
715 Matsumura, K., & Hyon, S. H. (2009). Polyampholytes as low toxic
716 efficient cryoprotective agents with antifreeze protein properties.
717 *Biomaterials*, *30*(27), 4842–4849.
718 https://doi.org/10.1016/j.biomaterials.2009.05.025
719 Matsumura, K., Nakajima, N., Sugai, H., & Hyon, S. H. (2014). Self-
720 degradation of tissue adhesive based on oxidized dextran and poly-l-
721 lysine. *Carbohydrate Polymers*, *113*, 32–38.
722 https://doi.org/10.1016/j.carbpol.2014.06.073
723 Matsumura, K., & Rajan, R. (2021). Oxidized Polysaccharides as Green
724 and Sustainable Biomaterials. *Current Organic Chemistry*, *25*.
725 https://doi.org/10.2174/1385272825666210428140052
726 McGrath, R. (1972). Protein measurement by ninhydrin determination of
727 amino acids released by alkaline hydrolysis. *Analytical Biochemistry*,
728 *49*(1), 95–102. https://doi.org/10.1016/0003-2697(72)90245-X
729 Mehvar, R. (2000). Dextrans for targeted and sustained delivery of
730 therapeutic and imaging agents. In *Journal of Controlled Release* (Vol.
731 69, Issue 1, pp. 1–25). Elsevier. https://doi.org/10.1016/S0168-
732 3659(00)00302-3
733 Mizuno, Y., Mizuta, R., Hashizume, M., & Taguchi, T. (2017). Enhanced
734 sealing strength of a hydrophobically-modified Alaska pollock gelatin-
735 based sealant. *Biomaterials Science*, *5*(5), 982–989.
736 https://doi.org/10.1039/c6bm00829a
737 Mo, X., Iwata, H., Matsuda, S., & Ikada, Y. (2000). Soft tissue adhesive
738 composed of modified gelatin and polysaccharides. *Journal of*

Biomaterials Science, Polymer Edition, *11*(4), 341–351. https://doi.org/10.1163/156856200743742

Munechika, K., Sogame, Y., Kishi, N., Kawabata, Y., Ueda, Y., Yamanouchi, K., & Yokoyama, K. (1994). Tissue Distribution of Macromolecular Conjugate, Adriamycin Linked to Oxidized Dextran, in Rat and Mouse Bearing Tumor Cells. *Biological and Pharmaceutical Bulletin*, *17*(9), 1193–1198. https://doi.org/10.1248/bpb.17.1193

Naitoh, Y., Kawauchi, A., Kamoi, K., Soh, J., Okihara, K., Hyon, S. H., & Miki, T. (2013). Hemostatic effect of new surgical glue in animal partial nephrectomy models. *Urology*, *81*(5), 1095–1100. https://doi.org/10.1016/j.urology.2013.01.002

Nonsuwan, P., Matsugami, A., Hayashi, F., Hyon, S. H., & Matsumura, K. (2019). Controlling the degradation of an oxidized dextran-based hydrogel independent of the mechanical properties. *Carbohydrate Polymers*, *204*, 131–141. https://doi.org/10.1016/j.carbpol.2018.09.081

Nonsuwan, P., & Matsumura, K. (2019). Amino-Carrageenan@Polydopamine Microcomposites as Initiators for the Degradation of Hydrogel by near-Infrared Irradiation for Controlled Drug Release. *ACS Applied Polymer Materials*, *1*(2), 286–297. https://doi.org/10.1021/acsapm.8b00209

Ono, K., Saito, Y., Yura, H., Ishikawa, K., Kurita, A., Akaike, T., & Ishihara, M. (2000). Photocrosslinkable chitosan as a biological adhesive. *Journal of Biomedical Materials Research*, *49*(2), 289–295.

Ortel, T. L., Charles, L. A., Keller, F. G., Marcom, P. K., Oldham, H. N., Kane, W. H., & Macik, B. G. (1994). Topical thrombin and acquired coagulation factor inhibitors: Clinical spectrum and laboratory diagnosis. *American Journal of Hematology*, *45*(2), 128–135. https://doi.org/10.1002/ajh.2830450206

Ramond, M. J., Valla, D., Gotlib, J. P., Rueff, B., & Benhamou, J. P. (1986). OBTURATION ENDOSCOPIQUE DES VARICES OESO-GASTRIQUES PAR LE BUCRYLATE®. I: ETUDE CLINIQUE DE 49 MALADES. *Gastroenterologie Clinique et Biologique*, *10*(8–9), 575–579. https://europepmc.org/article/med/3491014

Reyes, J. M. G., Herretes, S., Pirouzmanesh, A., Wang, D. A., Elisseeff, J. H., Jun, A., McDonnell, P. J., Chuck, R. S., & Behrens, A. (2005). A

775 modified chondroitin sulfate aldehyde adhesive for sealing corneal
776 incisions. *Investigative Ophthalmology and Visual Science*, *46*(4),
777 1247–1250. https://doi.org/10.1167/iovs.04-1192
778 Sakai, S., Tsumura, M., Inoue, M., Koga, Y., Fukano, K., & Taya, M.
779 (2013). Polyvinyl alcohol-based hydrogel dressing gellable on-wound
780 via a co-enzymatic reaction triggered by glucose in the wound exudate.
781 *Journal of Materials Chemistry B*, *1*(38), 5067–5075.
782 https://doi.org/10.1039/c3tb20780c
783 Siedentop, K. H., Park, J. J., Shah, A. N., Bhattacharyya, T. K., &
784 O'Grady, K. M. (2001). Safety and efficacy of currently available
785 fibrin tissue adhesives. *American Journal of Otolaryngology-Head and*
786 *Neck Medicine and Surgery*, *22*(4), 230–235.
787 https://doi.org/10.1053/ajot.2001.24817
788 Silver, F. H., Wang, M. C., & Pins, G. D. (1995). Preparation and use of
789 fibrin glue in surgery. In *Biomaterials* (Vol. 16, Issue 12, pp. 891–
790 903). Elsevier. https://doi.org/10.1016/0142-9612(95)93113-R
791 Silverstein, S. C., Steinman, R. M., & Cohn, Z. A. (1977). Endocytosis. In
792 *Annual review of biochemistry* (Vol. 46, pp. 669–722). Annual
793 Reviews 4139 El Camino Way, P.O. Box 10139, Palo Alto, CA
794 94303-0139, USA .
795 https://doi.org/10.1146/annurev.bi.46.070177.003321
796 Sloan, J. W., Alexander, B. H., Lohmar, R. L., Wolff, I. A., & Rist, C. E.
797 (1954). Determination of Dextran Structure by Periodate Oxidation
798 Techniques. *Journal of the American Chemical Society*, *76*(17), 4429–
799 4434. https://doi.org/10.1021/ja01646a045
800 Takagi, K., Araki, M., Fukuoka, H., Takeshita, H., Hidaka, S., Nanashima,
801 A., Sawai, T., Nagayasu, T., Hyon, S. H., & Nakajima, N. (2013).
802 Novel powdered anti-adhesion material: Preventing postoperative
803 intra-abdominal adhesions in a rat model. *International Journal of*
804 *Medical Sciences*, *10*(4), 467–474. https://doi.org/10.7150/ijms.5607
805 Takagi, K., Tsuchiya, T., Araki, M., Yamasaki, N., Nagayasu, T., Hyon, S.
806 H., & Nakajima, N. (2013). Novel biodegradable powder for
807 preventing postoperative pleural adhesion. *Journal of Surgical*
808 *Research*, *179*(1), e13–e19. https://doi.org/10.1016/j.jss.2012.01.056
809 Thornalley, P. J. (1993). The glyoxalase system in health and disease. In
810 *Molecular Aspects of Medicine* (Vol. 14, Issue 4, pp. 287–371).

Pergamon. https://doi.org/10.1016/0098-2997(93)90002-U
Tressl, R., Nittka, C., Kersten, E., & Rewicki, D. (1995). Formation of Isoleucine-Specific Maillard Products from [1-13C]-d-Glucose and [1-13C]-d-Fructose. *Journal of Agricultural and Food Chemistry*, *43*(5), 1163–1169. https://doi.org/10.1021/jf00053a009
Wallace, D. G., Cruise, G. M., Rhee, W. M., Schroeder, J. A., Prior, J. J., Ju, J., Maroney, M., Duronio, J., Ngo, M. H., Estridge, T., & Coker, G. C. (2001). A tissue sealant based on reactive multifunctional polyethylene glycol. *Journal of Biomedical Materials Research*, *58*(5), 545–555. https://doi.org/10.1002/jbm.1053
Wells-Knecht, K. J., Zyzak, V., Litchfield, J. E., Thorpe, S. R., & Baynes, J. W. (1995). Mechanism of Autoxidative Glycosylation: Identification of Glyoxal and Arabinose as Intermediates in the Autoxidative Modification of Proteins by Glucose1". In *Biochemistry* (Vol. 34). https://pubs.acs.org/sharingguidelines
You, K. E., Koo, M. A., Lee, D. H., Kwon, B. J., Lee, M. H., Hyon, S. H., Seomun, Y., Kim, J. T., & Park, J. C. (2014). The effective control of a bleeding injury using a medical adhesive containing batroxobin. *Biomedical Materials (Bristol)*, *9*(2), 025002. https://doi.org/10.1088/1748-6041/9/2/025002
Yu, R. J., & Bishop, C. T. (1967). Novel oxidations of methyl glycopyranosides by periodic acid in dimethyl sulfoxide. *Canadian Journal of Chemistry*, *45*(19), 2195–2203. https://doi.org/10.1139/v67-355